Revised **Ms. No. REAC-D-22-00382**

Oxidation of hexacyanoferrate(II) ion by hydrogen peroxide: inhibition by polyalcohols and related compounds

Joaquin F. Perez-Benito [iD] · **Pol Prado-Diaz**

Joaquin F. Perez-Benito

jfperezdebenito@ub.edu

ORCID [iD]

J. F. Perez-Benito: 0000-0001-8407-3458

Departamento de Ciencia de Materiales y Quimica Fisica, Seccion de Quimica Fisica, Facultad de Quimica, Universidad de Barcelona, Marti i Franques 1, 08028 Barcelona, Spain

Abstract

The oxidation of hexacyanoferrate(ll) ion by a large excess of hydrogen peroxide, in slightly acidic aqueous media containing potassium dihydrogen phosphate (pH 5.10 ± 0.05), was followed by monitoring the increase of absorbance at 420 nm as the colorless Fe(ll) complex gradually evolved into the yellow Fe(lll) complex. The reaction was inhibited by OH-containing organic compounds, either alcohols or carbohydrates, and two different inhibition pathways were observed, an iron(III)-independent pathway (rate constant k_1) and an iron(III)-mediated pathway (rate constant k_2). A BASIC-language computer program was developed in order to use the fourth-order Runge-Kutta integration method to obtain the concentrations of the Fe(ll)-inhibitor complex and the Fe(lll) reaction product. Rate constant k_1, whose value is determined by that of the initial rate, decreased slightly as the concentration of alcohol / carbohydrate increased, and a mechanism involving the formation of hydroxyl radicals in a Fenton-like reaction and its posterior scavenging by the organic antioxidant additive has been proposed. Of the 8 inhibiting agents that were tried, the most potent antioxidant under the experimental conditions of this study was D-mannitol. Rate constant k_2, whose value is a measurement of the deviation from a pseudo-first order behavior provoked by the inhibiting agent, increased notably as the concentration of the latter increased, and a mechanism involving the complexation of the Fe(lll) product by the organic inhibitor and its posterior outer-sphere one electron reduction from hexacyanoferrate(ll) ion has also been proposed. This might result in a blockage of the regeneration of pentacyanoaquaferrate(ll) ion, an intermediate believed to be essential for the redox reaction to take place.

Keywords Carbohydrates · Hexacyanoferrate(II) ion · Hydrogen peroxide · Hydroxyl radical intermediate · Inhibition· Polyalcohols

Introduction

The oxidation of hexacyanoferrate(II) ion by hydrogen peroxide, following the overall stoichiometry:

$$2[Fe^{II}(CN)_6]^{4-} + H_2O_2 + 2H^+ \longrightarrow 2[Fe^{III}(CN)_6]^{3-} + 2H_2O \qquad (1)$$

has puzzled chemical kinetics workers for decades because of its complexity and lack of a good reproducibility. This anomalous behavior is thought to be caused by the hydrolysis of the initial hexacyano complex [1], involving the replacement of a cyanide ligand by a water molecule to yield an aquapentacyano species:

$$[Fe^{II}(CN)_6]^{4-} + H_2O \rightleftharpoons [Fe^{II}(CN)_5(H_2O)]^{3-} + CN^- \qquad (2)$$

Given that the hydrolyzed complex is known to react with hydrogen peroxide much faster than the non-hydrolyzed one, the initial rate of the redox reaction shows a strong dependence on the time elapsed between the preparation of the reductant aqueous solution and the beginning of the kinetic process. Moreover, the fact that Eq. 2 presents a notable photochemical activation [2] makes the reproducibility problems even worse, since the initial rate depends also on the illumination of the laboratory when the experiment is performed.

On the other hand, the reactions of hydrogen peroxide with metal ions and their complexes are interesting, not only from the point of view of pure chemistry but also because of the biological implications. Actually, hydrogen peroxide is one of the metabolites formed inside the cells of aerobic organisms after the oxygen uptake, its reactions with transition metal ions

in their lower oxidation states leading to the formation of the extremely dangerous hydroxyl free radicals [3 – 5]:

$$M^{z+} + H_2O_2 \longrightarrow M^{(z+1)+} + HO^- + HO^{\cdot} \quad (3)$$

whereas its reactions with transition metal ions in their higher oxidation states lead to the formation of the also dangerous superoxide radicals [6 – 8]:

$$M^{(z+1)+} + H_2O_2 \longrightarrow M^{z+} + 2H^+ + O_2^{\cdot -} \quad (4)$$

the metal M usually being either Fe (Eq. 3 called then the Fenton reaction [9 – 14]) or Cu (Eq. 3 known then as a Fenton-like reaction [15 – 17]).

Since iron(lll) salts are insoluble in all but very acidic aqueous media, the addition of an appropriate ligand such as cyanide ion presents the advantage of keeping the oxidation product of Fe(ll) in solution [18]. In particular, the reaction between hexacyanoferrate(ll) and hydrogen peroxide has been reported to be strongly inhibited by well-known chelating agents as EDTA and oxalate ion [19]. Although the authors interpreted their results assuming that the inhibitors act as scavengers of trace metal impurities that would play the role of catalysts, this would be tantamount to accepting that the reaction in the absence of those impurities would be almost non-existing, and other interpretations are indeed possible. We intend to work starting from a different hypothesis: complexation of either the reactant hexacyanoferrate(II) ion or the reaction product hexacyanoferrate(III) ion by the added inhibiting agent precludes the formation of pentacyanoaquaferrate(II) ion, $[Fe(CN)_5(H_2O)]^{3-}$ (see Eq. 2), the latter complex being suspected to be an essential intermediate for the oxidation by hydrogen peroxide to take place. In the case of the reaction product, that formation would presumably occur by Fe(II)-Fe(III) direct outer-sphere electron transfer [20 – 22]:

$$[Fe^{II}(CN)_6]^{4-} + [Fe^{III}(CN)_5(H_2O)]^{2-} \longrightarrow [Fe^{III}(CN)_6]^{3-} + [Fe^{II}(CN)_5(H_2O)]^{3-} \quad (5)$$

Thus, if pentacyanoaquaferrate(III) ion is formed as a reaction product, Eq. 5 leads to the regeneration of the active form of the reducing agent, pentacyanoaquaferrate(II) ion.

Actually, EDTA and other chelating agents are used in medicine to treat the morbidity and mortality due to the iron overload syndrome, such as the one resulting from frequent and long-term blood transfusions to remediate the anemia observed in thalassemia patients [23 – 26]. This therapeutic effect might be related to the inhibition of the intracellular Fe(ll)-hydrogen peroxide reaction (Eq. 3), thus preventing the formation of hydroxyl free radicals.

In the present work, we will try to substantiate the alternative hypotheses consisting in the complexation of either Fe(ll) or Fe(lll) by the chelating agent. To that end, a kinetic study of the inhibiting effect exerted by several polyalcohols and other related compounds on the title reaction will be carried out.

Experimental

Materials and methods

All the experiments were done using as solvent water previously purified by deionization followed by treatment with a Millipore Synergy UV system (milli-Q quality, κ = 0.05 μS/cm at 25.0ºC). The reactants required to carry out the redox reaction were potassium hexacyanoferrate(II) trihydrate: $K_4[Fe(CN)_6]\cdot 3H_2O$ (Merck) as reducing agent and hydrogen peroxide: H_2O_2 (Sigma-Aldrich) as oxidizing agent. Other chemicals used were potassium hexacyanoferrate(III): $K_3[Fe(CN)_6]$ (Merck) to study the potential effect of the oxidation product at the beginning of the redox process and potassium dihydrogenphosphate: KH_2PO_4

(Merck) as a source of hydrogen ions for the acid-catalyzed reaction. The compounds tried as possible inhibitors were methanol: CH_3OH (Sigma-Aldrich) and the polyalcohols 1,2-ethanediol: CH_2OH-CH_2OH (ethylene glycol, Sigma-Aldrich), 1,2,3-propanetriol: CH_2OH-$CHOH$-CH_2OH (glycerol, glycerine, Sigma-Aldrich), 1,2,3,4-butanetetrol: CH_2OH-$(CHOH)_2$-CH_2OH (L-threitol, Sigma-Aldrich), 1,2,3,4,5-pentanepentol: CH_2OH-$(CHOH)_3$-CH_2OH (adonitol, Sigma-Aldrich) and 1,2,3,4,5,6-hexanehexol: CH_2OH-$(CHOH)_4$-CH_2OH (D-mannitol, Sigma-Aldrich), as well as the carbohydrates of the monosaccharide type α-D-glucopyranose: $C_6H_{12}O_6$ (D-glucose, dextrose, Sigma-Aldrich) and of the disaccharide type β-D-Fructofuranosyl α-D-glucopyranoside: $C_{12}H_{22}O_{11}$ (sucrose, Sigma-Aldrich).

Instrumentation

The pH measurements were done by means of a Wave pH-meter, provided with a digital presentation until the second decimal figure (± 0.01 pH) and a combination electrode, calibrated with the aid of commercial buffers of known pH (4.00 and 7.00, Sigma-Aldrich). The temperature was kept constant by means of a thermostatic bath provided with a digital reading (± 0.1 ºC). The kinetic runs were followed measuring periodically the absorbances at 420 nm with a Shimadzu 160 A double beam UV-Vis spectrophotometer (± 0.001 *A*), using a quartz cell of 1 cm optical path length. At that wavelength both reactants hexacyanoferrate(ll) ion and hydrogen peroxide are transparent (yielding a colorless solution) but the oxidation product hexacyanoferrate(lll) ion shows an absorption peak (ε = 1015 M^{-1} cm^{-1} [27], yielding a yellow solution).

Kinetic experiments

The reducing agent, Fe(II), was the last reactant to be added (1 mL of the desired concentration) to a thermostated aqueous solution containing all the other required chemicals (24 mL), and its solution (in previously thermostated water) was prepared right before the reaction started. The total volume of the reaction mixtures was thus fixed at a constant value in all the experiments (25 mL). In order to avoid as much effect of the laboratory illumination on the reaction rate as possible, aluminum foil was used to wrap around all the 1-mL pipette, the 50-mL volumetric flask containing the Fe(ll) solution and the 100-mL Erlenmeyer flask containing the reacting mixture. The oxidizing agent, hydrogen peroxide, was always in great excess with respect to the reducing one, hexacyanoferrate(ll) ion (isolation method). The absorbances were periodically measured (time interval: 10 s) during 16 minutes (99 values). In total, 255 kinetic runs were performed.

Results and discussion

Experimental absorbance-time plots

The profiles of the *A*(420) vs. *t* plots obtained when monitoring the formation of the reaction product, Fe(lll), showed a downward-concave curvature due to the rate decrease caused by the decay of the concentration of the limiting reactant, Fe(ll). The plots recorded in the initial absence of Fe(lll) revealed also that the inhibiting agent (in this case D-mannitol) had little effect on the initial rate, but the inhibition was more pronounced as the reaction advanced (Fig. 1), suggesting that the oxidation product, hexacyanoferrate(lll) ion, had an important contribution to the experimentally observed effect. This was confirmed by performing some

kinetic runs in the initial presence of Fe(lll), revealing that addition of the polyalcohol managed then to slow down the reaction from its very beginning (Fig. 2).

Kinetic model for the inhibited reaction: differential equations

Some trials have been made in order to explain the inhibition experimental data. The one for which the best results were obtained was based on the following simplified mechanism:

$$Fe^{II} \xrightarrow[H_2O_2]{k_I} Fe^{III} \quad (6)$$

$$Fe^{III} + ROH \underset{}{\overset{K_{II}}{\rightleftharpoons}} Fe^{III} - ROH \quad (7)$$

$$Fe^{II} + Fe^{III} - ROH \xrightarrow{k_{III}} Fe^{III} + Fe^{II} - ROH \quad (8)$$

In Eq. 6 we have schematically represented the oxidation of hexacyanoferrate(ll) ion by hydrogen peroxide (yielding a hydroxyl free radical and a hydroxide ion). On the other hand, Eq. 7 corresponds to the complexation of the hexacyanoferrate(lll) ion formed in the previous reaction by the OH-containing (either alcohol or carbohydrate) species used as inhibiting agent, whereas in Eq. 8 we have the outer-sphere transfer of one electron from iron(ll) to the iron(lll)-inhibitor complex to yield and iron(ll)-inhibitor complex. This model mechanism assumes that the latter complex does not react with hydrogen peroxide, at least not as readily as the free, non-ROH complexed iron(ll) species does.

The differential kinetic equation associated with Eq. 6 can be written as:

$$v_I = k_I [Fe^{II}] \quad (9)$$

Equation 7 can be treated as a quasi-equilibrium [28] provided it is fast enough in both directions in comparison to the global hexacyanoferrate(ll) ion-hydrogen peroxide redox reaction (condition indeed fulfilled given that Eq. 6 is a slow step). This leads to the following differential equation for the step represented in Eq. 8:

$$v_{III} = \frac{K_{II}\, k_{III}\, [Fe^{II}]\, [Fe^{III}]_T\, [ROH]}{1 + K_{II}\, [ROH]} \quad (10)$$

where the total concentration of iron(lll) (free form + complexed form), the one experimentally accessible from the absorbance readings, is calculated as:

$$[Fe^{III}]_T = [Fe^{III}] + [Fe^{III} - ROH] \quad (11)$$

Kinetic model for the inhibited reaction: point-by-point numerical integration

Equations 9 and 10 can be rewritten as:

$$v_I = k_1\, [Fe^{II}] \quad (12)$$

$$v_{III} = k_2\, [Fe^{II}]\, [Fe^{III}]_T \quad (13)$$

where the concentrations on the right side of the equations are only those changing with time, one decreasing and the other increasing, whilst the symbols k_1 and k_2 are used with the objective to discern between what we could call microscopic rate constants (k_I and k_{III}) and the macroscopic ones, the latter being given by:

$$k_1 = k_I \quad (14)$$

$$k_2 = \frac{K_{II}\, k_{III}\, [ROH]}{1 + K_{II}\, [ROH]} \quad (15)$$

k_1 being a pseudo-first order rate constant (in s^{-1}) since it depends on the initial concentration of hydrogen peroxide (in large excess), whereas k_2 is a pseudo-second order rate constant (in $M^{-1}\ s^{-1}$) provided the inhibitor ROH is also in large excess.

An approximate point-by-point integration procedure (fourth-order Runge-Kutta method [29]) was implemented with the aim of obtaining the values of the concentration of the iron(ll)-inhibitor complex and that of the total concentration of iron(lll). The concentration of free iron(ll), the only one assumed to react with hydrogen peroxide and required in Eqs. 12 and 13, was then obtained as:

$$[Fe^{II}] = [Fe^{II}]_o - [Fe^{III}]_T - [Fe^{II} - ROH] \quad (16)$$

The absorbance of the reacting mixture at 420 nm could be deduced by application of the Beer-Lambert law to the light-absorbing species at that wavelength, the reaction product iron(III):

$$A_\lambda = \varepsilon_\lambda [Fe^{III}]_T\, l \quad (17)$$

where ε_λ is the molar absorption coefficient and *l* the optical path length.

A computer program was written in BASIC language to perform the required calculations. In this program two main subroutines were coded, one in charge of the numerical integration of the differential equations (Eqs. 12 and 13), and the other starting with some trial values of three fitting parameters, the initial absorbance and the two macroscopic rate constants ($A_{\lambda,o}$, k_1 and k_2), and varying them systematically until the best fit was found. This was defined as the one that minimized the average error given by:

$$E = \frac{\sum_{i=1}^{N} \left| A_{i,cal} - A_{i,exp} \right|}{N} \quad (18)$$

where $A_{i,cal}$ and $A_{i,exp}$ are the calculated and experimental values of the absorbance at different instants during the course of the reaction, respectively, and N = 25 is the number of absorbance-time couples of experimental data recorded for each kinetic run. The program so developed yielded a good concordance between the calculated and experimental absorbances. Actually, depending on the experimental conditions, the average error spanned within the range $E = (2.20 - 6.81) \times 10^{-4}$.

In a typical kinetic run, performed in the presence of D-mannitol as inhibitor, the concordance between the theoretical and experimental absorbances was excellent ($E = 3.06 \times 10^{-4}$) provided the fit was limited to the first 4 minutes (N = 25 points), although a clear deviation could be observed afterwards, since the extrapolated theoretical rate decreased much faster than the experimental one (Fig. 3). This divergence between theoretical model and experiment suggests that the Fe(ll)-inhibitor complex formed in Eq. 8 can also react with hydrogen peroxide, but with a rate constant much lower than that corresponding to the inhibitor-free Fe(ll) complex (k_I, Eq. 6). Alternatively, the reaction depicted in Eq. 8 could be reversible, although with a rate in the backward direction much lower than that in the forward one. However, given the difficulty of obtaining reproducible kinetic measurements that is inherent to the hexacyanoferrate(ll)-hydrogen peroxide reaction (due to the photochemical replacement of a cyanide ligand by a water molecule), the use of a three-parameter mathematical model makes more sense than the use of one involving an excessive number of

fitting parameters (that would certainly oversize the accidental random errors), even if the former should be considered just as a reasonable approximation to the real kinetic behavior.

Determination of equilibrium constant K_{II}

The log k_2 vs. log $[ROH]_o$ linear plots yielded slopes within the 0 < slope < 1 range in the eight cases that were studied. This result suggested a complexation of Fe(III) by the organic compound, so that the lower the value of the slope the higher the corresponding value of the associated equilibrium constant. Taking logarithms in Eq. 15, an easy mathematical transformation leads to:

$$\log \left\{ k_2 \left(1 + K_{II} [ROH]\right)\right\} = \log \left(K_{II}\, k_{III}\right) + \log [ROH] \qquad (19)$$

Thus, provided we know the value of equilibrium constant K_{II}, a graphical representation of the left-hand side of Eq. 19 as a function of the logarithm of the inhibiting agent concentration should yield a linear plot with a slope equal to 1. Different values of that equilibrium constant were tried in a systematic way until the desired slope was attained. This fact allowed us to obtain K_{II} for the different inhibiting agents that were tried.

Inhibition effect: kinetic study

The effect of six alcohols (methanol, ethylene glycol, glycerol, L-threitol, adonitol and D-mannitol and two carbohydrates (D-glucose and sucrose) on the rate of hexacyanoferrate(II)-hydrogen peroxide reaction was investigated. Whereas rate constant k_1 decreased slightly in all eight cases as shown for the case of D-mannitol (Fig. 4, top), rate constant k_2 increased

notably (Fig. 4, bottom). Since, given their corresponding definitions, k_1 favors the hexacyanoferrate(II)-hydrogen peroxide reaction, whereas k_2 opposes to that process, both behaviors indicate the existence of a kinetic inhibition by the OH-containing organic compound. Thus, the effect on k_1 corresponded to an iron(III)-independent inhibition pathway, whereas that on k_2 corresponded to an iron(III)-mediated inhibition pathway.

A series of experiments with a variable initial concentration of D-mannitol was performed with the reaction product, hexacyanoferrate(lll) ion, already present at the beginning of the kinetic runs. The resulting double logarithm plots indicated a more pronounced decrease of rate constant k_1 (slope: − 0.073 ± 0.009) than when Fe(lll) was initially absent (slope: − 0.041 ± 0.005), as shown in Fig. 5, top. With respect to k_2, the increase observed with increasing alcohol concentration when Fe(lll) was initially absent (slope: 0.45 ± 0.05) seemed to fade away when hexacyanoferrate(lll) ion was added to the reactant mixture at $t = 0$, so that a horizontal straight line was obtained (slope: − 0.01 ± 0.02), as can be seen in Fig. 5, bottom.

The values obtained for the slopes of the log k_1 vs. log $[ROH]_o$ and log k_2 vs. log $[ROH]_o$ linear plots, slope (k_1) and slope (k_2), as well as those obtained for the equilibrium constant K_{II} and the microscopic rate constant k_{III} are compiled in Table 1. Despite the considerable magnitude of the experimental errors associated with those parameters, it seemed that slope (k_1) decreased with an increase of the number of carbon atoms in the inhibiting agent molecule (Fig. 6, top), whereas K_{II} increased (Fig. 6, middle) and k_{III} was essentially independent of that number (Fig. 6, bottom). The high random errors observed in this study were a direct result of the degree of irreproducibility coming from the photochemical hydrolysis of the hexacyanoferrate(II) ion to yield the active reducing agent,

pentacyanoaquaferrate(II) ion, rendering difficult to reproduce an exact initial concentration of the latter.

Iron(III)-independent inhibition pathway: mechanistic interpretation

In order to explain the otherwise minor decreasing effect exerted by the alcohol / carbohydrate inhibiting agent on the initial reaction rate through rate constant k_1, we need to postulate the following set of elementary chemical steps:

$$[Fe^{II}(CN)_6]^{4-} + H_3O^+ \xrightarrow{k_{IV}} [Fe^{II}(CN)_5(H_2O)]^{3-} + HCN \quad (20)$$

$$[Fe^{II}(CN)_5(H_2O)]^{3-} + H_2O_2 \xrightarrow{k_V} [Fe^{III}(CN)_5(H_2O)]^{2-} + HO^{\bullet} + HO^- \quad (21)$$

$$HO^{\bullet} + [Fe^{II}(CN)_6]^{4-} \xrightarrow[H^+]{k_{VI}} [Fe^{III}(CN)_5(H_2O)]^{2-} + CN^- \quad (22)$$

$$HO^{\bullet} + RHOH \xrightarrow{k_{VII}} H_2O + R^{\bullet}OH \quad (23)$$

$$R^{\bullet}OH + [Fe^{II}(CN)_6]^{4-} \xrightarrow[H^+]{k_{VIII}} RHOH + [Fe^{III}(CN)_6]^{3-} \quad (24)$$

$$R^{\bullet}OH + H_2O_2 \xrightarrow{k_{IX}} RHOH + HO_2^{\bullet} \quad (25)$$

$$2HO_2^{\bullet} \xrightarrow{k_X} H_2O_2 + O_2 \quad (26)$$

The reaction proposed in Eq. 20 is consistent with the available experimental information on the dramatic enhancement of the reaction rate resulting from the substitution of a cyanide ligand by a water molecule in the reactant complex [2]. Equation 21 is a typical Fenton-like reaction yielding a hydroxyl free radical [15 – 17]. We have also proposed a competition between hexacyanoferrate(ll) ion [30] (Eq. 22) and the organic compound tested as inhibiting agent (Eq. 23) to reduce the previously formed and highly oxidizing hydroxyl radical in two

parallel reactions. In the latter, the hydrogen atom transferred from the alcohol / carbohydrate to the hydroxyl radical is preferentially that bonded to the carbon atom supporting the OH group, so that a secondary carbon-based free radical is formed [31]. Again, we have proposed two new parallel reactions in which hexacyanoferrate(ll) ion (Eq. 24) and hydrogen peroxide (Eq. 25) compete to reduce the organic free radical. The latter yields the hydroperoxyl radical (protonated form of the superoxide radical) that dismutates in the final step (Eq. 26) [32, 33].

By application of the steady state approximation to the free radicals involved in the mechanism, the equation obtained for the pseudo-first order rate constant is:

$$k_1 = \frac{1}{[Fe^{II}(CN)_6{}^{4-}]_T} \frac{d\,[Fe^{III}]}{d\,t} = \alpha_H\, k_V\, [H_2O_2] \left(1 + \frac{w_1}{w_2}\right) \qquad (27)$$

with:

$$w_1 = k_{VI}\, [Fe^{II}(CN)_6{}^{4-}] + \frac{k_{VII}\, k_{VIII} [Fe^{II}(CN)_6{}^{4-}]\, [RHOH]}{k_{VIII} [Fe^{II}(CN)_6{}^{4-}] + k_{IX} [H_2O_2]} \qquad (28)$$

$$w_2 = k_{VI}\, [Fe^{II}(CN)_6{}^{4-}] + k_{VII}\, [RHOH] \qquad (29)$$

Now, taking the limit values of the pseudo-first order rate constant:

$$\lim_{[RHOH] \to 0} k_1 = 2\, \alpha_H\, k_V\, [H_2O_2] \qquad (30)$$

$$\lim_{[RHOH] \to \infty} k_1 = \alpha_H\, k_V\, [H_2O_2] \left\{1 + \frac{k_{VIII} [Fe^{II}(CN)_6{}^{4-}]}{k_{VIII} [Fe^{II}(CN)_6{}^{4-}] + k_{IX} [H_2O_2]}\right\} \qquad (31)$$

The fraction placed within the curly brackets is indeed a dimensionless number whose value falls in the range between 0 and 1, meaning that:

$$\alpha_H \, k_V \, [H_2O_2] \; < \; \lim_{[RHOH] \to \infty} k_1 \; < \; 2 \, \alpha_H \, k_V \, [H_2O_2] \qquad (32)$$

Therefore, Eq. 27 predicts a decrease of the pseudo-first order rate constant as the concentration of the RHOH species increases (inhibition effect). However, according to Eq. 32, this effect is expected to be of a very small magnitude (never reaching a 50% decrease in the value of k_1 even at an infinite concentration of the organic additive), in consonance with the small negative values given in Table 1 for the slopes of the log k_1 vs. log $[ROH]_o$ plots.

We have thus explained the inhibition exerted by the alcohol / carbohydrate agent through the pseudo-first order rate constant k_1 by the antioxidant power of that organic compound. Actually, the ability of D-mannitol to act as an efficient hydroxyl radical scavenger is well known [34 – 36]. The second order rate constant reported for Eq. 23 with this alcohol is k_{VII} = (1.88 ± 0.14) × 10^9 M^{-1} s^{-1} (in pulse radiolysis experiments with X-ray decomposition of hydrogen peroxide) [37], whereas that of Eq. 22 is k_{VI} = 1.1 × 10^{10} M^{-1} s^{-1} [38]. This means that, at the concentrations used in the present study, D-mannitol could successfully compete with hexacyanoferrate(ll) ion as a scavenger of the hydroxyl radicals.

Iron(III)-mediated inhibition pathway: mechanistic interpretation

The experimental information revealed that the tested alcohols and carbohydrates were more efficient as inhibitors when the product hexacyanoferrate(lll) ion was present in the reacting mixture. In order to explain this finding, our mechanism proposal consists of the following steps (in fair concordance with those assumed in the mathematical model used to obtain the kinetic data, Eqs. 6 – 8):

$$[Fe^{II}(CN)_6]^{4-} + [Fe^{III}(CN)_5(H_2O)]^{2-} \rightarrow [Fe^{III}(CN)_6]^{3-} + [Fe^{II}(CN)_5(H_2O)]^{3-} \quad (33)$$

$$[Fe^{III}(CN)_5(H_2O)]^{2-} + ROH \rightleftarrows [Fe^{III}(CN)_5(ROH)]^{2-} + H_2O \quad (34)$$

$$[Fe^{II}(CN)_6]^{4-} + [Fe^{III}(CN)_5(ROH)]^{2-} \rightarrow [Fe^{III}(CN)_6]^{3-} + [Fe^{II}(CN)_5(ROH)]^{3-} \quad (35)$$

In this way, in the absence of any alcohol / carbohydrate inhibitor additive, when hexacyanoferrate(II) ion transfers one electron to pentacyanoaquaferrrate(lll) ion (formed as reaction product in Eqs. 21 and 22) in an outer-sphere redox reaction the hydrolyzed form of the iron(ll) reactant complex is regenerated (Eq. 33). However, when the iron(lll) product is previously complexed by the organic compound (Eq. 34), the outer-sphere electron transfer does not result in the formation of the active form of the reducing agent capable of reacting with hydrogen peroxide, the hydrolyzed iron(ll) complex (Eq. 35).

Hence, according to the proposed mechanism (Eqs. 33 – 35), the role of the inhibiting agent in the reaction is that of preventing the fast regeneration of the pentacyanoaquaferrate(II) ion once the latter is consumed by oxidation with hydrogen peroxide, so that the kinetic profile will deviate more and more from a pseudo-first order behavior as the reaction advances. This results in the reaction rate decreasing much faster than expected for a pseudo-first order kinetics, and in a value of k_2 greater than zero and increasing with the inhibiting agent concentration, when Fe(III) was initially absent from the reaction mixture (Fig. 4, bottom), as well as in the decrease of k_1 being more pronounced than usual when Fe(III) was initially present (Fig. 5, top).

However, although the complexation mechanism (Eqs. 33 – 35) was the one to give the best concordance with the experimental data among the different kinetic models that were

tried, a certain contribution of a free radical mechanism cannot be completely discarded. This would take place through the reaction between the superoxide radicals formed in Eq. 25 as intermediates and the Fe(III) complexes formed as reaction products [39]:

$$HO_2^{\bullet} + Fe^{III} \longrightarrow O_2 + H^+ + Fe^{II} \quad (36)$$

Thus, the sequence given by Eqs. 23, 25 and 36 would result in the regeneration of the reactant Fe(II) and could explain, at least partially, the inhibition caused by the organic additives in the presence of Fe(III).

References

1 Baxendale JH (1952) Decomposition of hydrogen peroxide by catalysts in homogeneous aqueous solution. Adv Catal 4:31 – 86

2 Perez-Benito JF, Pages-Rebull J (2021) Oxidation of hexacyanoferrate(II) ion by hydrogen peroxide: Evidence of free radical intermediacy. React Kinet Mech Catal 133:631 – 653

3 Galano A (2008) Carbon nanotubes as free-radical scavengers. J Phys Chem C 112:8922 – 8927

4 Korotkova EI, Misini B, Dorozhko EV, Bukkel MV, Plotnikov EV, Linert W (2011) Study of OH radicals in human serum blood of healthy individuals and those with pathological schizophrenia. Int J Mol Sci 12:401 – 409

5 Matros A, Peshev D, Peukert M, Mock H, Van den Ende W (2015) Sugars as hydroxyl radical scavengers: Proof-of-concept by studying the fate of sucralose in Arabidopsis. Plant J 82:822 – 839

6 Fridovich I (1997) Superoxide anion radical (O_2^-), superoxide dismutases, and related matters. J Biol Chem 272:18515 – 18517

7 Nikoli-Kokic A, Blagojevic D, Spasic MB (2010) Complexity of free radical metabolism in human erythrocytes. J Med Biochem 29:189 – 195

8 Fridovich I (2013) Oxygen: How do we stand it? Med Princ Pract 2:131 – 137

9 Weiss J, Humphrey CW (1949) Reaction between hydrogen peroxide and iron salts. Nature 163:691

10 Barb WG, Baxendale JH, George P, Hargrave KR (1949) Reactions of ferrous and ferric ions with hydrogen peroxide. Nature 163:692 – 694

11 Barb WG, Baxendale JH, George P, Hargrave KR (1951) Reactions of ferrous and ferric ions with hydrogen peroxide. I. The ferrous ion reaction. Trans Faraday Soc 47:462 – 500

12 Edwards JO, Curci R (1992) In: Strukul G (ed) Catalytic oxidation with hydrogen peroxide as oxidant. Kluwer, Dordrecht

13 Sawyer DT, Sobkowiak A, Matsushita, T (1996) Metal [ML_x, M = Fe, Cu, Co, Mn]/hydroperoxide-induced activation of dioxygen for the oxygenation of hydrocarbons: Oxygenated Fenton chemistry. Acc Chem Res 29:409 – 416

14 Li Y, Yuan J, Fang Y (2022) Iron(II) immobilized within a metal−organic framework mixed-matrix membrane as a H_2O_2 turn-on sensor. Inorg Chem 61:3103 – 3110

15 Pandey NK, Li HB, Chudal L, Bui B, Amador E, Zhang MB, Yu HM, Chen ML, Luo X, Chen W (2022) Exploration of copper-cysteamine nanoparticles as an efficient heterogeneous Fenton-like catalyst for wastewater treatment. Mater Today Phys 22:100587

16 Alley KR, Gavenda-Eaton TR, Prieto-Centurion D (2022) Photo-thermal catalytic degradation of organophosphate simulant over Cu, Co, and Fe on titania. Catal Commun 162:106369

17 Arezou F, Marcello B, Alireza K, Gilles M (2022) $Fe_{25}Co_{03}Zn_{02}O_4$/CuCr-LDH as a visible-light-responsive photocatalyst for the degradation of caffeine, bisphenol A, and simazine in pure water and real wastewater under photo-Fenton-like degradation process. Chemosphere 291:132920

18 Baltpurvins KA, Burns RC, Lawrance GA, Stuart AD (1997) Effect of Ca^{2+}, Mg^{2+}, and anion type on the aging of iron(III) hydroxide precipitates. Environ Sci Techol 31:1024 – 1032

19 Bray DG, Thompson RC (1994) Trace metal ion catalysis in the oxidation of $Fe(CN)_6^{4-}$ by H_2O_2. Inorg Chem 33:905 – 909

20 Atwood JD, Corrainepandolfino MS, Zhen YQ, Striejewske WS, Ang P (1994) Electron-transfer reactions of metal-carbonyl anions. J Coord Chem 32:65 – 78

21 Zhang SW, Adrian L, Schuurmann G (2021) Outer-sphere electron transfer does not underpin B-12-dependent olefinic reductive dehalogenation in anaerobes. Phys Chem Chem Phys 23:27520 – 27524

22 Lesanavicius M, Boucher JL, Cenas N (2022) Reactions of recombinant neuronal nitric oxide synthase with redox cycling xenobiotics: A mechanistic study. Int J Mol Sci 23:980

23 Weiner M (1964) Factors influencing clinical use of chelates in iron storage disease. Ann N Y Acad Sci 119:789 – 796

24 Born T, Kontoghiorghe CN, Spyrou A, Kolnagou A, Kontoghiorghes GJ (2013) EDTA chelation reappraisal following new clinical trials and regular use in millions of

patients: Review of preliminary findings and risk/benefit assessment. Toxicol Mech Methods 23:11 – 17

25 Song YZ, Huang ZJ, Song Y, Tian QJ, Liu XR, She ZN, Jiao J, Lu E, Deng YH (2014) The application of EDTA in drug delivery systems: Doxorubicin liposomes loaded via NH_4EDTA gradient. Int J Nanomedicine 9:3611 – 3621

26 Zhou X, Huang L, Wu J, Qu Y, Jiang H, Zhang J, Qiu S, Liao C, Xu X, Xia J, Lian Q (2022) Impaired bone marrow microenvironment and stem cells in transfusion-dependent beta-thalassemia. Biomed Pharmacother 146:112548

27 Katafias A, Impert O, Kita P (2008) Hydrogen peroxide as a reductant of hexacyanoferrate(III) in alkaline solutions: Kinetic studies. Transition Met Chem 33:1041 – 1046

28 Perez-Benito JF (2017) Some considerations on the fundamentals of chemical kinetics: Steady state, quasi-equilibrium, and transition state theory. J Chem Educ 94:1238 – 1246

29 Espenson JH (1995) Chemical kinetics and reaction mechanisms. McGraw-Hill, New York

30 Perez-Benito JF (2004) Iron(lll)-hydrogen peroxide reaction: Kinetic evidence of a hydroxyl-mediated chain mechanism. J Phys Chem A 108:4853 – 4858

31 Walling C (1998) Intermediates in the reactions of Fenton type reagents. Acc Chem Res 31:155 – 157

32 Sawyer DT, Valentine JS (1981) How super is superoxide? Acc Chem Res 14:393 – 400

33 Hullar T, Anastasio C (2011) Yields of hydrogen peroxide from the reaction of hydroxyl radical with organic compounds in solution and ice. Atmos Chem Phys 11:7209 – 7222

34 Mohamadin AM (2001) Possible role of hydroxyl radicals in the oxidation of dichloroacetonitrile by Fenton-like reaction. J Inorg Biochem 84:97 – 105

35 Xu H, Zhu Y, Cui D, Du M, Wang J, Ma R, Jiao Z (2019) Evaluating the roles of OH radicals, H_2O_2, ORP and pH in the inactivation of yeast cells on a tissue model by surface micro-discharge plasma. J Phys D: Appl Phys 52:395201

36 Ma S, Lee S, Kim K, Im J, Jeon H (2021) Purification of organic pollutants in cationic thiazine and azo dye solutions using plasma-based advanced oxidation process via submerged multi-hole dielectric barrier discharge. Sep Purif Technol 255:117715

37 Luliano L, Patrico D, Ghiselli A, Bonativa MS, Violi F (1992) Reaction of dipyridamole with the hydroxyl radical. Lipids 27:349 – 353

38 Goldstein S, Czapski G (1997) Indirect oxidation of ferrocyanide by peroxynitrite – Evidence against the formation of hydroxyl radicals. Nitric Oxide 1:417 – 422

39 Rabai G, Kustin K, Epstein IR (1989) Systematic design of chemical oscillators. 57. Light-sensitive oscillations in the hydrogen peroxide oxidation of ferrocyanide. J Am Chem Soc 111:8271 – 8273

Table 1 Kinetic parameters for eight different inhibiting agents[a]

Inhibitor	Slope (k_1)[b]	Slope (k_2)[c]	K_{II}[d] / 10^3 M^{-1}	k_{III}[e] / M^{-1} s^{-1}
Methanol	- 0.021 ± 0.005	0.38 ± 0.07	1.2 ± 0.3	12 ± 6
Ethylene glycol	- 0.023 ± 0.003	0.27 ± 0.06	2.3 ± 0.6	7 ± 3
Glycerol	- 0.023 ± 0.003	0.31 ± 0.04	2.1 ± 0.5	9 ± 4
L-Threitol	- 0.024 ± 0.006	0.47 ± 0.05	1.2 ± 0.3	12 ± 3
Adonitol	- 0.017 ± 0.004	0.30 ± 0.02	2.8 ± 0.5	12 ± 3
D-Mannitol	- 0.041 ± 0.005	0.45 ± 0.05	1.0 ± 0.2	21 ± 7
D-Glucose	- 0.029 ± 0.003	0.32 ± 0.04	1.2 ± 0.2	12 ± 3
Sucrose	- 0.025 ± 0.002	0.25 ± 0.06	2.3 ± 0.6	7 ± 3

[a] $[K_4Fe(CN)_6]_o = 1.97 \times 10^{-4}$ M, $[H_2O_2]_o = 7.83 \times 10^{-2}$ M, $[KH_2PO_4] = 1.44 \times 10^{-2}$ M, pH 5.10 ± 0.05, 25.0 °C

[b] Slopes of the log k_1 vs. log $[ROH]_o$ linear plots

[c] Slopes of the log k_2 vs. log $[ROH]_o$ linear plots

[d] Equilibrium constant associated with Eq. 7

[e] Rate constant associated with Eq. 8

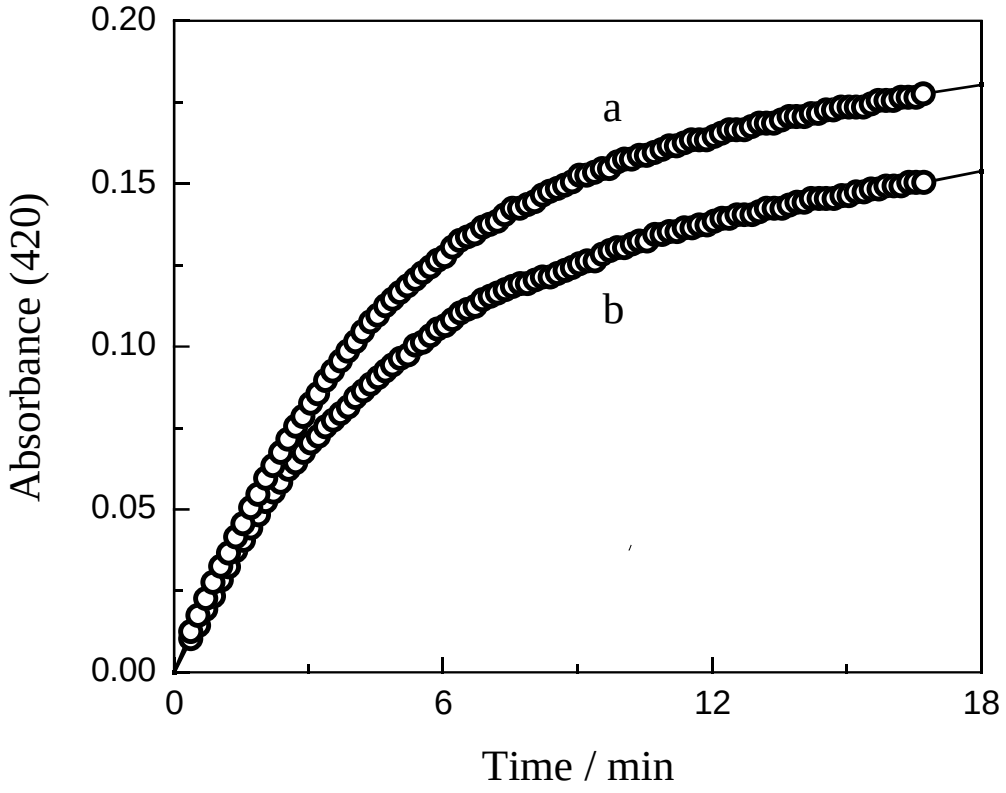

Fig. 1 Absorbance at 420 nm as a function of time for the reaction carried out at $[K_3Fe(CN)_6]_o$ = 0 in the absence (a) and presence (b) of D-mannitol (167×10^{-2} M) $[K_4Fe(CN)_6]_o = 1.97 \times 10^{-4}$ M, $[H_2O_2]_o = 7.83 \times 10^{-3}$ M, $[KH_2PO_4]_o = 1.44 \times 10^{-2}$ M, pH 5.10 ± 005, 25.0ºC

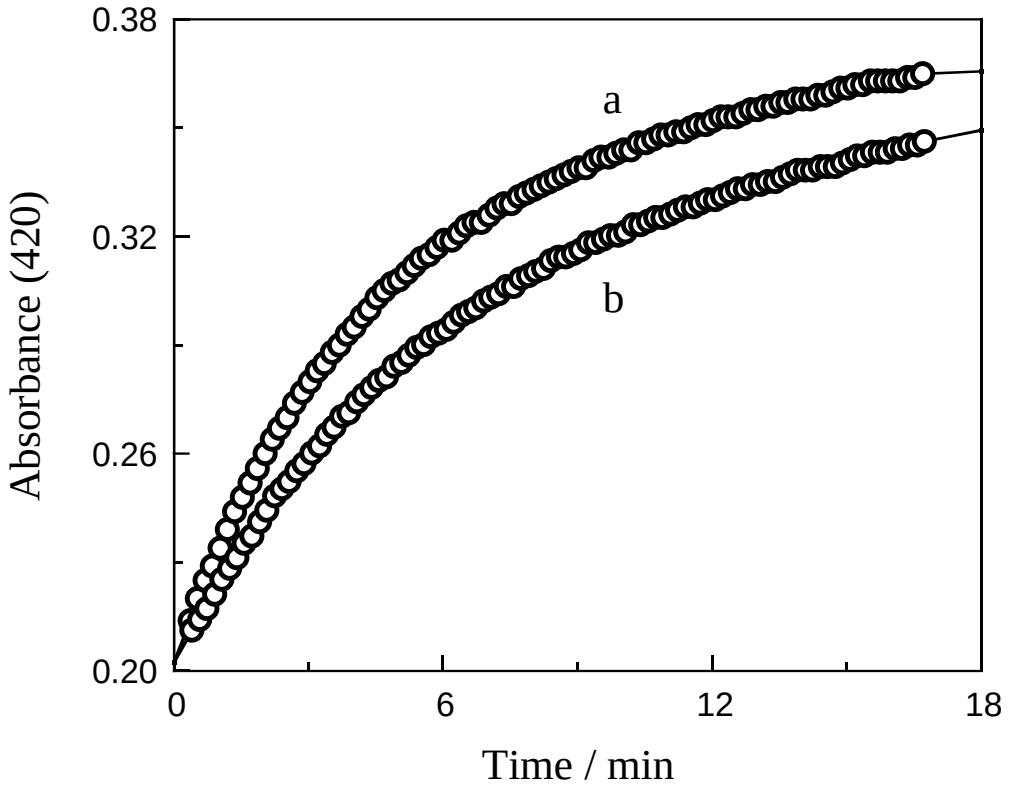

Fig. 2 Absorbance at 420 nm as a function of time for the reaction carried out at $[K_3Fe(CN)_6]_o = 1.97 \times 10^{-4}$ M in the absence (a) and presence (b) of D-mannitol (1.67×10^{-2} M) $[K_4Fe(CN)_6]_o = 1.97 \times 10^{-4}$ M, $[H_2O_2]_o = 7.83 \times 10^{-3}$ M, $[KH_2PO_4]_o = 1.44 \times 10^{-2}$ M, pH 5.10 ± 005, 25.0ºC

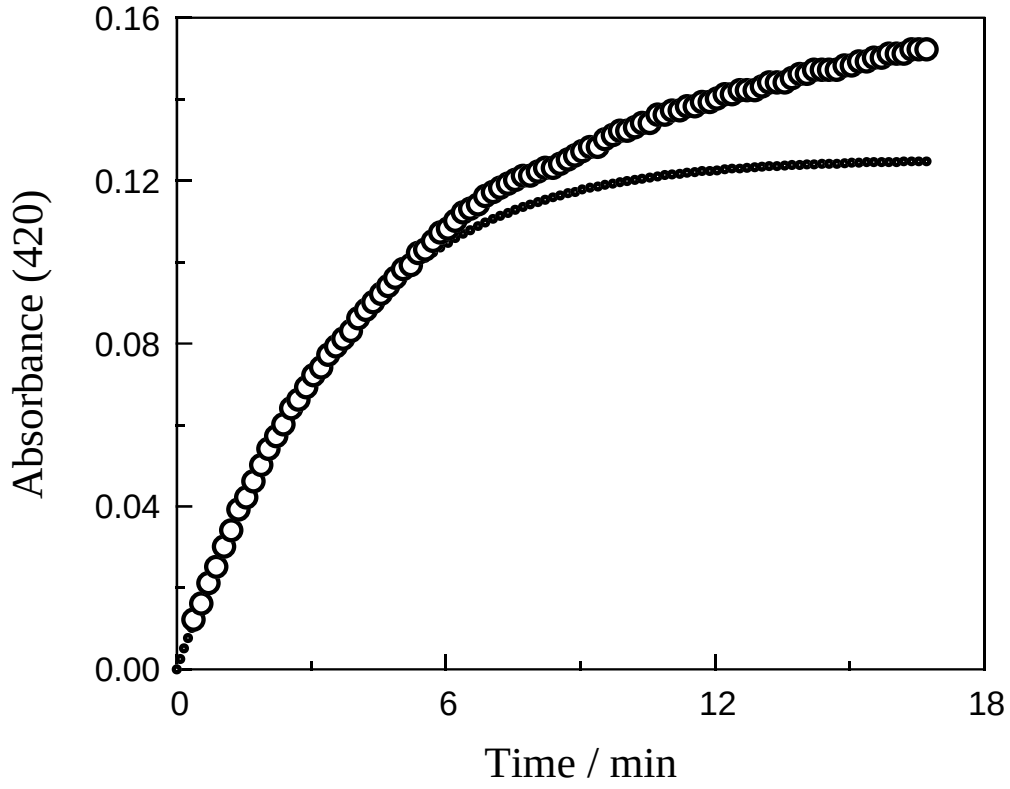

Fig. 3 Absorbance at 420 nm as a function of time during the course of the reaction showing the experimental (circles) and theoretical (dots) values. $[K_4Fe(CN)_6]_o$ = 1.97 × 10^{-4} M, $[H_2O_2]_o$ = 7.83 × 10^{-3} M, [D-mannitol]$_o$ = 1.67 × 10^{-2} M, $[KH_2PO_4]_o$ = 1.44 × 10^{-2} M, pH 5.10 ± 0.05, 25.0ºC

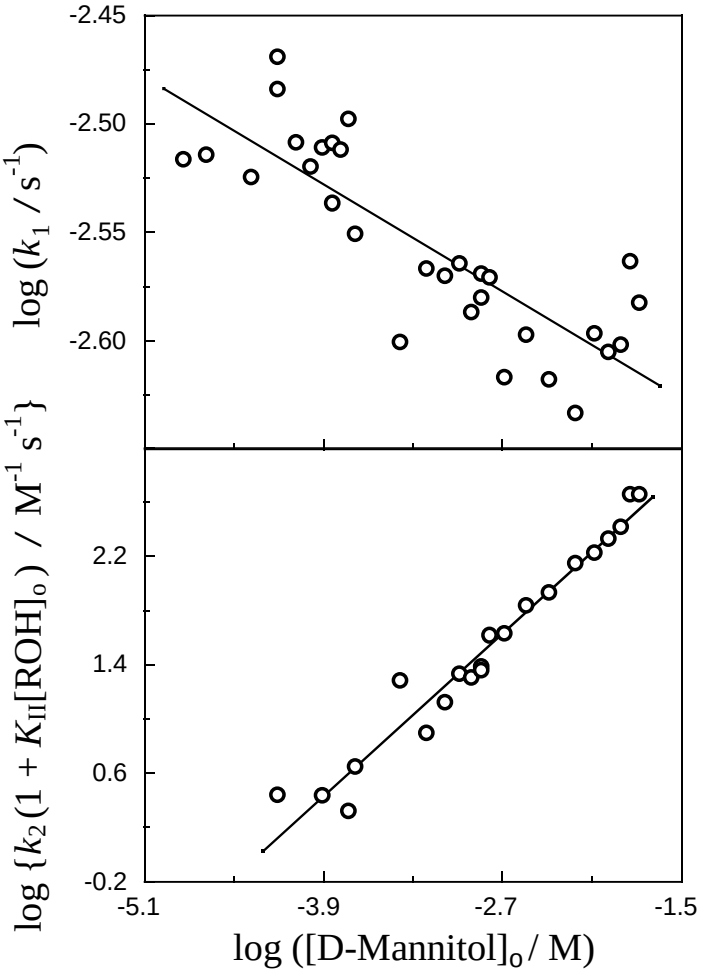

Fig. 4 Double logarithm plots for the dependences of rate constants k_1 (top) and k_2 (bottom) on the initial concentration of D-mannitol ($1.45 \times 10^{-5} - 1.66 \times 10^{-2}$ M). $[K_4Fe(CN)_6]_o = 1.97 \times 10^{-4}$ M, $[H_2O_2]_o = 7.83 \times 10^{-3}$ M, $[KH_2PO_4]_o = 1.44 \times 10^{-2}$ M, pH 5.10 ± 0.05, 25.0ºC

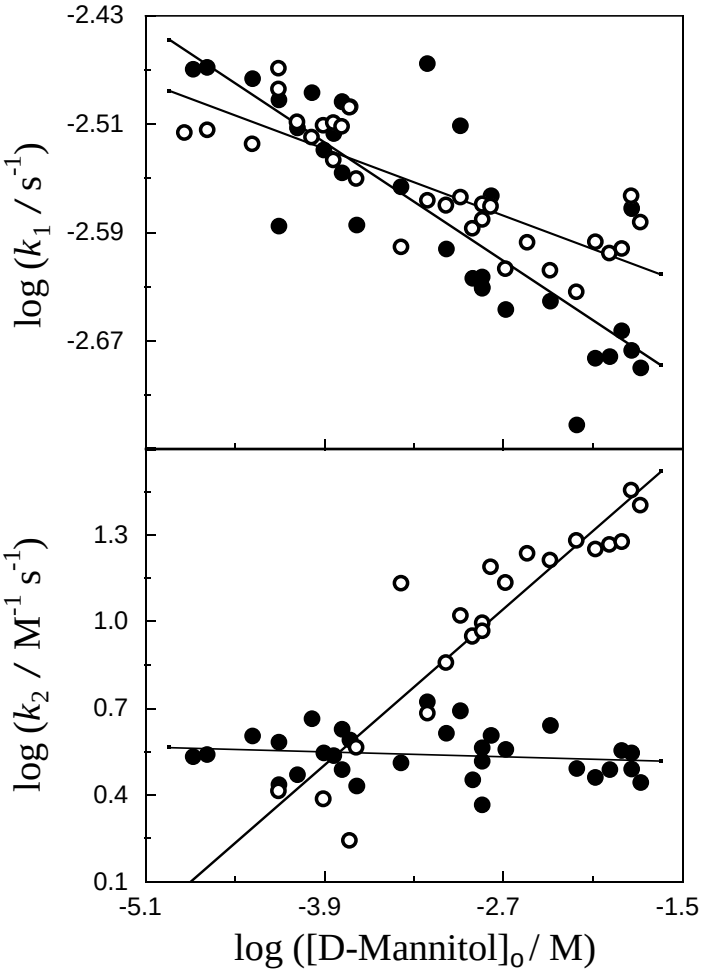

Fig. 5 Double logarithm plots for the dependences of rate constants k_1 (top) and k_2 (bottom) on the initial concentration of D-mannitol ($1.45 \times 10^{-5} - 1.67 \times 10^{-2}$ M). $[K_4Fe(CN)_6]_o = 1.97 \times 10^{-4}$ M, $[K_3Fe(CN)_6]_o = 0$ (empty circles) and 1.97×10^{-4} M (filled circles), $[H_2O_2]_o = 7.83 \times 10^{-3}$ M, $[KH_2PO_4]_o = 1.44 \times 10^{-2}$ M, pH 5.10 ± 0.05, 25.0ºC

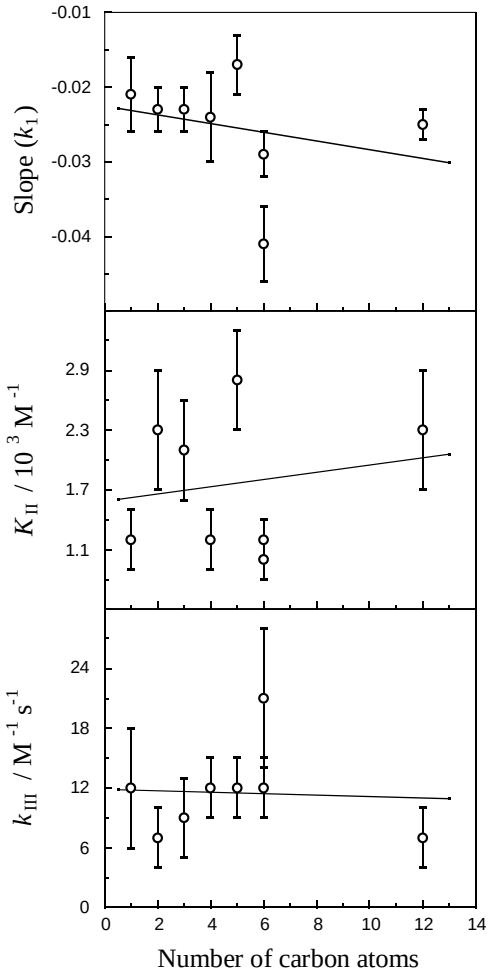

Fig. 6 Values of slope (k_1) (top), K_{II} (middle) and k_{III} (bottom) as a function of the number of carbon atoms of each inhibiting agent with accidental error bars. $[K_4Fe(CN)_6]_o = 1.97 \times 10^{-4}$ M, $[H_2O_2]_o = 7.83 \times 10^{-3}$ M, $[KH_2PO_4]_o = 1.44 \times 10^{-2}$ M, pH 5.10 ± 0.05, 25.0ºC